■ REVIEW ■

Clinical Applications of Long-Wavelength (1,000-nm) Optical Coherence Tomography

Pearse A. Keane, MRCOphth, MSc; Humberto Ruiz-Garcia, MD; Srinivas R. Sadda, MD

ABSTRACT

Commercial optical coherence tomography (OCT) instruments generally use light sources in the range of 800 to 860 nm. Although imaging with these light sources provides excellent visualization of the retinal architecture, details of structures and abnormalities below the retinal pigment epithelium are often limited. At the same time, the optimal light source wavelength for clinical OCT imaging is unknown. OCT imaging using longer wavelength light (1,050 nm) has several potential advantages, including less scattering with media opacity and deeper penetration. This article reviews the current state-of-the-art of long wavelength OCT imaging and explores potential clinical applications. **[Ophthalmic Surg Lasers Imaging 2011;42:S67-S74.]**

INTRODUCTION

Optical coherence tomography (OCT), first described by Huang et al. in 1991, is a new form of imaging analogous to ultrasonography but using light waves instead of sound.[1,2] With this modality, a light source is used to illuminate a tissue of interest and the time delay and intensity of the backscattered light is then measured using a process known as low coherence interferometry. In this manner, high-resolution cross-sectional (tomographic) images of ocular tissues, such as the neurosensory retina, may be constructed. Since 2002, with the commercial release of the Stratus system (Carl Zeiss Meditec, Dublin, CA), OCT imaging has been widely adopted by clinicians for the diagnosis and treatment of macular disease.[3] More recently, technical advances have resulted in the introduction, by multiple vendors, of next-generation commercial OCT systems (often termed spectral-domain OCT) that offer increased image acquisition speed, sensitivity, and resolution.[4,5] Although spectral-domain OCT systems use a different method of interferometry than older "time-domain" devices such as the Stratus OCT, they employ similar light sources—typically superluminescent diodes with wavelengths of approximately 800 nm.[6] Use of such wavelengths allows both spectral-domain and time-do-

From NIHR Biomedical Research Centre for Ophthalmology (PAK), Moorfields Eye Hospital NHS Foundation Trust and UCL Institute of Ophthalmology, London, United Kingdom; and Doheny Eye Institute (HR-G, SRS), Keck School of Medicine of the University of Southern California, Los Angeles, California.

Originally submitted February 2, 2011. Accepted for publication April 5, 2011.

This research has received a proportion of its funding from the Department of Health's NIHR Biomedical Research Centre for Ophthalmology at Moorfields Eye Hospital and UCL Institute of Ophthalmology. The views expressed in the publication are those of the authors and not necessarily those of the Department of Health.

Dr. Sadda is a co-inventor of Doheny Eye Institute intellectual property related to optical coherence tomography that has been licensed by Topcon Medical Systems, and is a member of the scientific advisory board for Heidelberg Engineering. Dr. Sadda also receives research support from Carl Zeiss Meditec, Optos, and Optovue, Inc. The remaining authors have no financial or proprietary interest in the materials presented herein.

Address correspondence and reprint requests to Srinivas R. Sadda, MD, Doheny Eye Institute-DEI 3623, 1450 San Pablo Street, Los Angeles, CA 90033. E-mail: ssadda@doheny.org

doi: 10.3928/15428877-20110627-06

main systems to provide detailed images of the neurosensory retina; however, visualization of areas beneath the retinal pigment epithelium (RPE) is more limited, a significant limitation given the known choroidal origin of many macular disorders. As a result, efforts have been underway to develop OCT systems that can use light sources with wavelengths of approximately 1,000 nm, often termed "long-wavelength" OCT. Such systems would allow enhanced retinal penetration of light and potentially improved visualization beyond the RPE.[3]

In this review, we begin by providing an overview of the physical principles underlying OCT, highlighting the effects of light source wavelength on image acquisition. We then describe the technology underlying prototype long-wavelength OCT platforms and early attempts at its clinical application.

EFFECTS OF LIGHT SOURCE WAVELENGTH IN OCT

Although OCT is analogous to ultrasonography, the use of light waves in OCT produces images with much greater resolution because the wavelength of light is many times less than that of sound.[2] However, the use of light instead of sound is challenging because the speed of light exceeds the speed of sound by a factor of 150,000, making direct measurements of optical "echoes" difficult. To overcome this hurdle, the principles of low coherence interferometry are used in OCT devices.[1]

In interferometry, the combination of light reflected from a tissue of interest and light reflected from a reference path produces characteristic patterns of interference that are dependent on the mismatch between the reflected waves.[7] Because the time delay and amplitude of one of the waves (ie, the reference path) are known, the mismatch information can be extracted from the interference pattern to deduce the time delay and amplitude of light returning from the sample tissue. In interferometry, interference will only be detected when the difference in path length between the light scattered from the tissue and light traveling in the reference path is less than the coherence length of the light source. Light with long coherence is used in conventional interferometry and typically produces interference over a distance of meters with relatively poor axial resolution. In OCT, light with low coherence is used; therefore, interference occurs only over very short distances and images with relatively high resolution can be produced. Low coherence light sources include superluminescent diodes (a type of super-bright light-emitting diode similar to the diode lasers used in compact disc players but made to emit over a wider range of wavelengths) or lasers with extremely short pulses (femtosecond lasers). The axial resolution of OCT images is dependent on the bandwidth of the light source used and the coherence length of the light source ("coherence gating"), which in turn is determined by the central wavelength. The transverse resolution of OCT is limited by the size of the light spot that can be focused on the retina ("confocal gating").[6]

Because the coherence length of a light source is dependent on the central wavelength of that light source, it would seem that OCT devices with lower central wavelengths would possess superior axial resolutions.[6] However, when lower light source wavelengths are employed, increased light scattering occurs in most tissues. Minimization of scattering is important to maximize the OCT signal, because it relies on the detection of light that has only been scattered by the structure of interest. Therefore, a central wavelength must be chosen to allow a good combination of high axial resolution and low scattering. In addition, absorption of light by the tissue of interest must also be considered; when light sources between 200 and 600 nm are used, tissue (oxy)-hemoglobin absorbs much of the incident light.[6]

Thus, commercial ophthalmic OCT devices have, to date, relied on light sources centered at approximately 800 nm. The Stratus OCT, for example, employs a superluminescent diode with a central wavelength of 820 nm and a bandwidth of 20 nm. This reliance is also related, in large part, to the easy availability of light source technology in this wavelength range. Ultrahigh-resolution OCT prototypes have been demonstrated that employ femtosecond light sources in the 650- to 950-nm range, but these currently remain prohibitively expensive and complex for inclusion in commercial instruments.[3]

OCT systems employing light sources with a central wavelength of approximately 800 nm provide images of the neurosensory retina such that all major intraretinal layers can be resolved, allowing a diverse range of clinical application.[4,5] However, the RPE is rich in melanin, a chromophore that is both highly scattering and highly absorbing.[8] As a result, there is limited penetration of light beyond this layer and it is difficult to visualize the choriocapillaris and choroid. Of note, the optical properties of melanin are highly wavelength dependent, with significantly decreased scattering and absorption for longer

wavelengths. In addition, scattering from lens opacity is also wavelength dependent, being markedly reduced at longer wavelengths.[9,10]

However, at these longer wavelengths, absorption of light by water places serious constraint on the wavelengths of light that can be used for macular OCT imaging (the human eye consists mainly of water, which is principally found in the cornea, lens, and vitreous).[11] Fortunately, the absorption spectrum of water contains two regions where light absorption is low (separated by an absorption peak at approximately 970 nm); one region is in the visible and near infrared light spectrum up to approximately 950 nm, the other is a band between 1,000 and 1,100 nm. Although water absorption between 1,000 and 1,100 nm remains higher than that at 800 nm, imaging at this wavelength is safer, with a higher upper limit for safe optical exposure (eg, the ANSI standard for permissible corneal exposure is five times higher in this wavelength range than at 800 nm).[12] Thus, the narrow band, between 1,000 and 1,100 nm, offers a window of opportunity for use as a light source in the next generation of OCT devices. Prototype devices have already been constructed employing this strategy and preliminary evidence suggests that they indeed allow greatly enhanced choroidal imaging (Fig. 1).

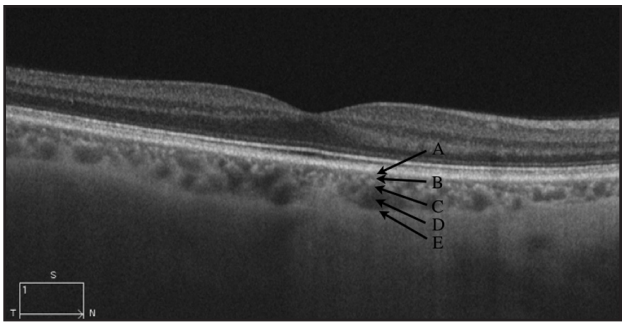

Figure 1. Optical coherence tomography (OCT) B-scan (512 A-scans over 6 mm, 4× averaged) image of a normal eye obtained using a prototype Carl Zeiss Meditec 1,050-nm spectral domain OCT (Dublin, CA). Note that the full-thickness of the choroid is visualized in addition to the internal aspect of the sclera. Bruch's membrane (A), choriocapillaris (B), Sattler's medium vessel layer (C), Haller's large vessel layer (D), and the sclerochoroidal interface (E) can be identified.

LONG-WAVELENGTH OCT TECHNOLOGY

Current commercially available, 800-nm, spectral-domain OCT systems employ spectrometers that typically consist of a collimating lens, a diffraction grating, and a high-speed, silicon, line-scan, charge coupled device (CCD) camera.[3,13,14] Light waves recombined in the interferometer pass into the spectrometer and are focused on the diffraction grating by the collimating lens. The light waves—with their interference patterns—are then dispersed in space; the resulting discrete packets of data can be analyzed using the CCD camera, with each pixel of the camera containing interferometric information from a discrete location within the retina). The speed at which interferometric signals can be transferred from the CCD camera is an important factor in determining the ultimate image acquisition speed of the device. In addition, the number of axial pixels in the OCT image is limited by the number of pixels on the CCD camera.

Although use of silicon-based CCD cameras has enabled major advances in commercial OCT instruments, such cameras are not currently sensitive enough, at wavelengths greater than 1,000 nm, to be incorporated into prototype long-wavelength OCT systems.[3] Long-wavelength OCT systems are more easily constructed using an alternative approach to image acquisition, so-called "swept-source" OCT.[15-18] Swept-source OCT systems employ a tunable laser (ie, one whose wavelength of operation can be altered in a controlled manner) and photodetectors in place of the silicon-based, line scan, CCD camera used in spectral-domain systems. When such systems employ a novel laser technique (termed Fourier-domain mode locking) images can be readily acquired at long wavelengths.[6] Furthermore, such swept-source systems often have image acquisition speeds in excess of 249,000 A-scans per second and have been described as "ultrahigh-speed" OCT.[16]

Although swept-source OCT systems offer many advantages, current prototypes are difficult to operate, expensive, and require complicated detection electronics.[19] In addition, they offer only limited optical bandwidth, usually centered on the shorter portion of the 1,060-nm wavelength band where melanin absorption is higher, and thus reducing the penetration and axial resolution of any resulting images.[19] In recent years, advances in CCD camera design have extended the possibility of long-wavelength OCT imaging using more conventional spectral-domain OCT methodologies. Although silicon-based cameras are not sensitive enough for such an approach, use of alternative semiconductors (such as indium–gallium–arsenide [InGaAs]) circumvents this barrier.[3] In the past, InGaAs cameras were slower and had reduced pixel densities compared to silicon-based CCD cameras. However, the recent availability of novel

TABLE
Specifications of Carl Zeiss Meditec Long-Wavelength Prototype

Variable	1,050-nm SD-OCT
Theoretical sensitivity	104.5 dB
Exp. sensitivity	~96.3 dB
Axial resolution (FWHM bandwidth)	8.4 µm (42.5 nm)
Detector	InGaAs camera
Speed (kHz)	47 to > 27
Pixels	1,024
Sensitivity roll-off	~6.3 dB/mm

SD-OCT = spectral-domain optical coherence tomography; FWHM = full-width at half-maximum; InGaAs = indium–gallium–arsenide.

InGaAs arrays, with unprecedented readout rates, has opened the possibility of commercial long-wavelength OCT systems.[19] The specifications of one such device, from Carl Zeiss Meditec, have recently been described (Table).

CLINICAL APPLICATIONS OF LONG-WAVELENGTH OCT

Following the widespread adoption of OCT imaging for the management of retinal diseases, it became increasingly important for retinal specialists to hone their understanding of both normal retinal anatomy and clinicopathologic correlations. Thus, it seems likely that the clinical application of long-wavelength OCT devices will stimulate a similarly increased awareness of choroidal-scleral structure.

The sclera is a largely avascular structure, consisting almost entirely of compact, interlacing bundles of collagen with small quantities of elastic tissue nearer the choroid.[20] The collagen bundles are 10- to 16-µm thick and 100- to 140-µm wide, run mostly parallel to the ocular surface, but cross each other in all directions. Between the choroid and the sclera is a thin "lamina fusca," consisting of closely packed lamellae of collagen fibers that run from the sclera anteriorly to the choroid; these lamellae adjoin potential spaces that may become evident when the layer becomes pathologically distended by serous fluid or hemorrhage ("suprachoroidal space").

The choroid itself is a largely vascular structure, surrounded by an elastic network in a net-like manner.[20] The short posterior ciliary arteries pierce and run through the sclera, forming an outer layer of large vessels in the choroid (Haller's layer). Medium-sized branches of these large vessels give rise to the middle, stromal layer of the choroid (Sattler's layer), before terminal arterioles give rise to an internal layer of capillary vessels (choriocapillaris). The choriocapillaris is divided into lobules, with each consisting of a central feeding arteriole, a capillary bed, and a series of peripheral draining venules. In addition to its prominent vessels, the choroidal stroma also contains numerous cells, including melanocytes, fibrocytes, and immune cells such as macrophages. The choroidal vasculature also shows a strikingly dense sympathetic and parasympathetic innervation. Finally, internal to the choriocapillaris is a non-cellular connective tissue layer (Bruch's membrane) that consists of two basal laminae, two collagen layers, and a single layer of elastin.[20]

Early long-wavelength OCT prototypes have been used to non-invasively delineate the choroidal vasculature. Povazay et al. have demonstrated high axial resolution (6.7 µm) OCT images, with penetration to the sclera, obtained at 1,060 nm using a three-dimensional OCT system with a high-speed (47,000 depth scans/sec) InGaAs camera.[19,21] Using this system, the authors were able to construct en face images where the structure of the choriocapillaris, Sattler's layer, Haller's layer, and choroidal–scleral interface could be clearly differentiated. Simultaneous reconstruction of the retinal microvasculature was also possible using this device. With optic nerve head scans, the fine structure of the lamina cribrosa and the circle of Zinn-Haller could also be seen.

Choroidal Thickness

Long-wavelength OCT devices may also facilitate accurate quantitative assessments of choroidal structure. On histology, choroidal thickness has typically been reported as between 170 and 220 µm.[20] However, accurate measurements of choroidal thickness are difficult in this context because histologic studies are often limited by artifact and shrinkage of tissue following tissue fixation. In addition, other factors, such as the continued circulation of blood, may be required to sustain the volume of the highly vascular choroidal tissue.[22] Studies using "enhanced depth imaging" OCT, a modified spectral-domain OCT scanning protocol where the device is adjusted to maximize its sensitivity at the choroid and B-scans are highly averaged, have allowed in vivo measurement of choroidal thickness.[23] In a normative study using enhanced depth imag-

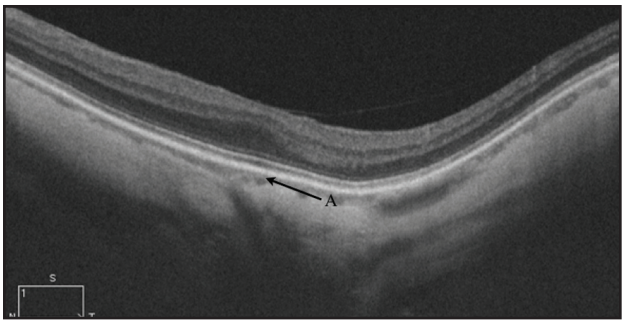

Figure 2. Optical coherence tomography (OCT) B-scan (512 A-scans over 6 mm, 4× averaged) image of a myopic eye (-9.00 diopter refraction and axial length of 27 mm) obtained using a prototype Carl Zeiss Meditec 1,050-nm spectral-domain OCT. The choroidal thickness is dramatically reduced (A).

ing OCT, choroidal thickness has been reported as thickest under the fovea (287 ± 76 µm), with significant decreases nasally (145 ± 57 µm at 3 mm nasal to the fovea).[24] However, larger values for subfoveal choroidal thickness have been reported recently using long-wavelength OCT prototypes. Esmaeelpour et al. reported a subfoveal choroidal thickness of 315 ± 106 µm in a cohort of normal subjects, with variations over the entire field of view.[25] Ikuno et al. reported values of 354 ± 111 µm for subfoveal choroidal thickness in healthy Japanese subjects.[26] Both studies have provided evidence that choroidal thickness decreases with increasing axial length, and preliminary clinical experience with 1,000-nm OCT suggests significant choroidal thinning may be present in patients with pathologic myopia (Fig. 2). Choroidal thickness may also be affected by age and refractive error.[26]

Cataract and Media Opacity

With the use of current, commercial 800-nm OCT devices, the presence of significant cataract or other media opacity can make image acquisition difficult.[27] Preliminary studies have demonstrated the clinical application of long-wavelength OCT devices for image acquisition in patients with significant lens opacity.[25,28] In particular, Esmaeelpour et al. investigated the effect of cataract grade on OCT retinal imaging quality. Their study demonstrated that in cataractous eyes, reduced signal strength was found in 65% of patients imaged with 800-nm OCT, but in only 10% of patients imaged with a 1,060-nm OCT prototype.[25]

Age-Related Macular Degeneration

Long-wavelength OCT devices are likely to greatly improve visualization of chorioretinal vascular disorders

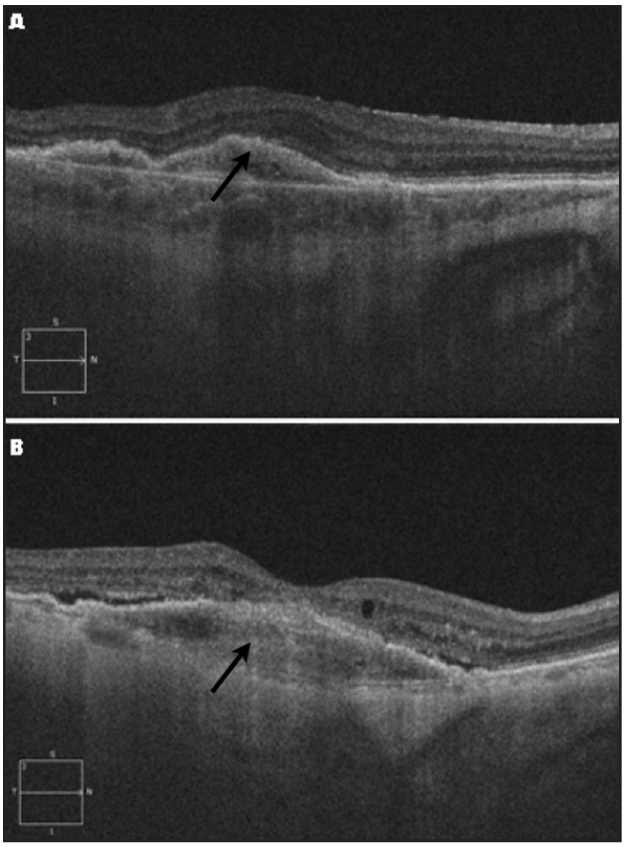

Figure 3. Optical coherence tomography (OCT) B-scans (512 A-scans over 6 mm, 4× averaged) from two different eyes (A and B) with neovascular age-related macular degeneration obtained using a prototype Carl Zeiss Meditec 1,050-nm spectral-domain OCT (Dublin, CA). Neovascular tissue (arrows) is visualized below the retinal pigment epithelium.

such as neovascular age-related macular degeneration. In particular, the detailed structural characteristics of pigment epithelium detachments have not been completely resolved, in large part due to the relative inability of commercially available OCT systems to visualize areas beneath the RPE.[5] Improved visualization of choroidal neovascularization, beneath the RPE, has now been reported in several long-wavelength OCT studies.[29,30] In many cases, fibrovascular pigment epithelium detachments can be seen to be occupied by solid layers of medium reflectivity material, separated by hyporeflective clefts—a finding consistent with histopathologic reports (Fig. 3).[31,32] In many serous pigment epithelium detachments, collections of solid material (the apparent fibrovascular proliferation) can be seen adherent to the outer surface of the RPE and associated with an underlying hyporeflective space (the serous fluid compartment). Long-wavelength OCT devices might also prove useful for the assessment of patients with

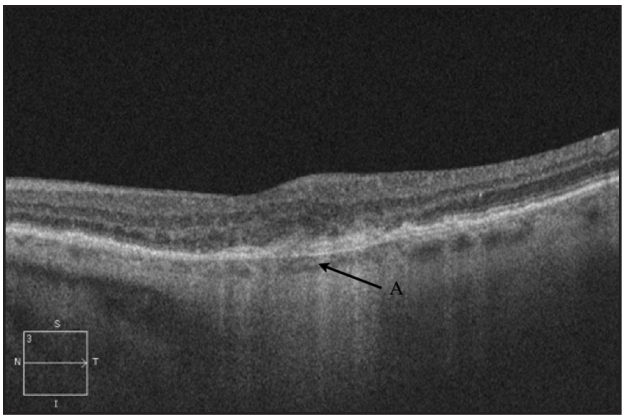

Figure 4. The 1,050-nm optical coherence tomography (OCT) B-scan (512 A-scans over 6 mm, 4× averaged) from the eye of an elderly patient with diminishing vision and macular pigmentary alterations but no typical drusen. OCT shows significant thinning of the choroid (A) and a diagnosis of age-related choroidal atrophy was made.

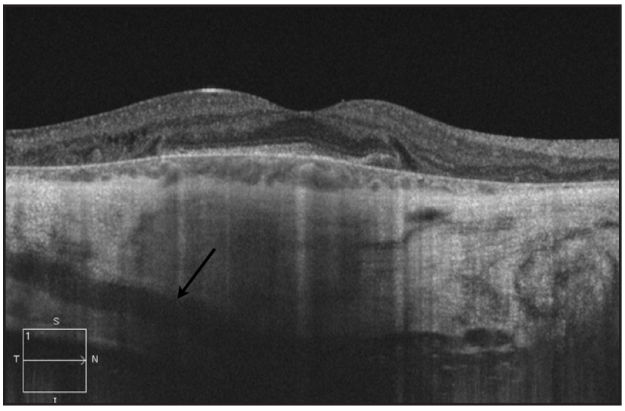

Figure 6. The 1,050-nm optical coherence tomography B-scan (512 A-scans over 6 mm, 4× averaged) from the eye of a patient with retinitis pigmentosa. The full extent of the choroid and sclera are visible in this eye. Vessels penetrating through the sclera are evident as linear hyporeflective structures (arrow).

"dry" age-related macular degeneration; such devices may allow early detection of choroidal neovascularization and highlight the role of age-related choroidal atrophy in visual loss (Fig. 4).[33]

Central Serous Chorioretinopathy

Using 800-nm OCT devices, central serous chorioretinopathy is typically seen as an area of serous retinal detachment accompanied by one or more discrete areas of pigment epithelium detachment.[34] More recently, enhanced depth imaging OCT protocols have demonstrated increased choroidal thickness in patients with central serous chorioretinopathy, a finding consistent with a pathogenic role for choroidal hyperpermeability.[35,36] It seems plausible that the differing proportions of subretinal and sub-RPE fluid seen in many cases of central serous chorioretinopathy may be related to differences in the functional and/or structural integrity of the RPE (occurring in the context of hyperpermeability). As such, the enhanced visualization of the RPE, Bruch's membrane, and choroid provided by long-wavelength OCT devices may provide new insights into the pathophysiology of this disorder (Fig. 5). Such insights may be applicable to other disorders with related features such as neovascular age-related macular degeneration and polypoidal choroidal vasculopathy.

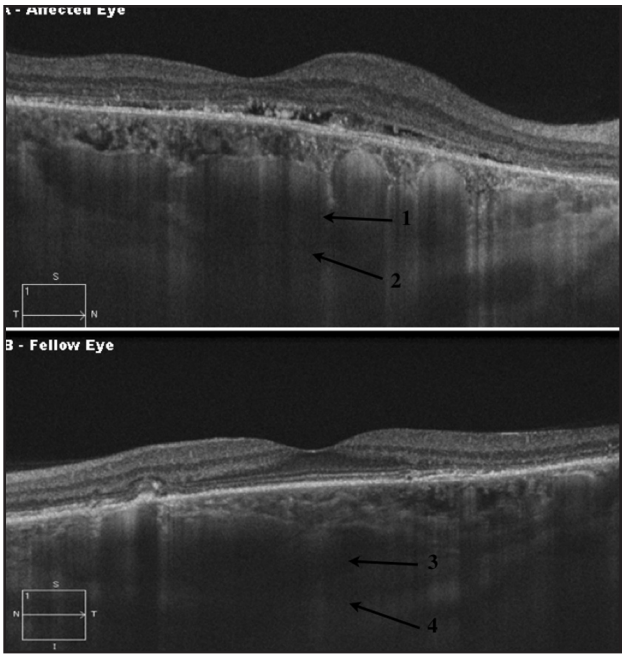

Figure 5. The 1,050-nm optical coherence tomography (OCT) B-scans (512 A-scans over 6 mm, 4× averaged) from both eyes of a patient with central serous chorioretinopathy. In the affected eye (A), the patient complained of visual blurring and distortion and subretinal fluid is evident. Both the affected eye and the asymptomatic fellow eye (B) show dramatic thickening of the choroid with marked dilation of the outermost choroidal vessels (Haller's layer) (1 and 3). Even with increased choroidal thickness, the sclerochoroidal (2 and 4) interface can be determined.

Other

Long-wavelength OCT devices have also been used to image choroidal structure in patients with uveitic disorders[37] and patients with inherited retinal degenerations such as retinitis pigmentosa (Fig. 6). Such devices may also prove useful for imaging of intraocular tumors. Traditionally, the diagnosis and longitudinal monitoring of choroidal tumors has been dependent on posterior seg-

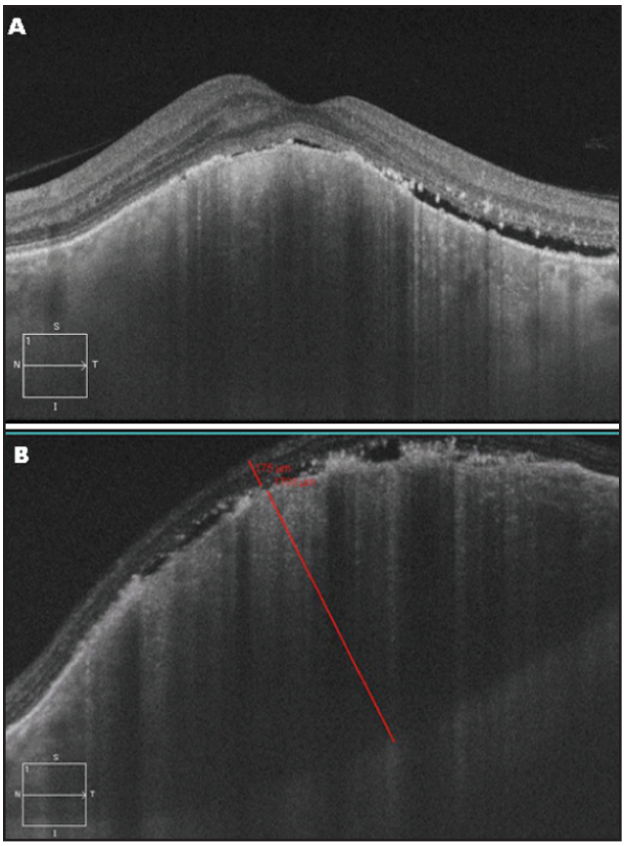

Figure 7. The 1,050-nm optical coherence tomography B-scans (512 A-scans over 6 mm, 4× averaged) from two different eyes (A and B) with small choroidal tumors. The tumors produce marked elevations of the retinal pigment epithelium and loss of the normal choroidal vascular pattern in the area of the tumor. Tumor thickness of greater than 1.6 mm could be measured (B).

ment ultrasonography[38]; for many posterior pole lesions, long-wavelength OCT imaging may provide supplementary information of clinical use (Fig. 7). As our ability to interpret choroidal images grows, and as long-wavelength OCT devices improve, such information could conceivably prove useful in determining the malignant potential of choroidal tumors. The use of 1,000-nm OCT systems may also prove useful for the evaluation of anterior segment morphology,[39] in particular the structures of the anterior chamber angle in the evaluation of patients with angle-closure glaucoma (Fig. 8).

CONCLUSION

Long-wavelength (1,000 nm) OCT expands the range of patients, structures, and diseases that may be amenable to OCT imaging. As long-wavelength OCT devices become incorporated into clinical practice, it

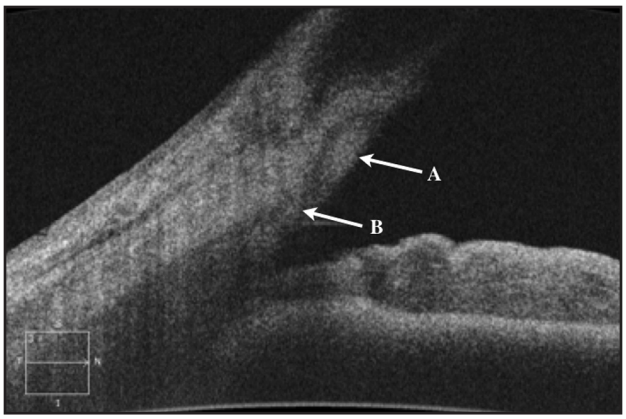

Figure 8. The 1,050-nm optical coherence tomography B-scan of the angle recess in a normal eye. The trabecular meshwork is clearly delineated (A). The sclera and choroid are also easily distinguished facilitating identification of the scleral spur (B).

is likely that clinicians will discover new anatomic features of chorioretinal disease, allowing increased understanding of disease pathophysiology and potentially improved patient treatment. In the future, because the longer wavelengths used in these devices do not stimulate retinal neurons, it may also be possible to use long-wavelength OCT systems as a means of probing the effects of retinal stimulation by other, shorter wavelength, visible light—a technique termed "optophysiology."[40] In addition, given that many swept-source OCT light sources (from manufacturers such as Exalos and Axsun) use the long end (1,050 to 1,310 nm) of the spectrum, 1,050-nm imaging may be an important component of future "ultrahigh-speed" OCT imaging.

REFERENCES

1. Huang D, Swanson EA, Lin CP, et al. Optical coherence tomography. *Science.* 1991;254:1178-1181.
2. Schuman JS, Puliafito CA, Fujimoto JG. *Optical Coherence Tomography of Ocular Diseases,* 2nd ed. Thorofare, NJ: SLACK Incorporated; 2004.
3. Drexler W, Fujimoto JG. State-of-the-art retinal optical coherence tomography. *Prog Retin Eye Res.* 2008;27:45-88.
4. Keane PA, Bhatti RA, Brubaker JW, Liakopoulos S, Sadda SR, Walsh AC. Comparison of clinically relevant findings from high-speed fourier-domain and conventional time-domain optical coherence tomography. *Am J Ophthalmol.* 2009;148:242-248.
5. Keane PA, Sadda SR. Imaging chorioretinal vascular disease. *Eye.* 2009;24:422-427.
6. van Velthoven MEJ, Faber DJ, Verbraak FD, van Leeuwen TG, de Smet MD. Recent developments in optical coherence tomography for imaging the retina. *Prog Retin Eye Res.* 2007;26:57-77.
7. Costa RA, Skaf M, Melo LA, et al. Retinal assessment using optical coherence tomography. *Prog Retin Eye Res.* 2006;25:325-353.
8. Wolbarsht ML, Walsh AW, George G. Melanin, a unique biological absorber. *Appl Opt.* 1981;20:2184-2186.
9. van den Berg TJ. Light scattering by donor lenses as a function of depth and wavelength. *Invest Ophthalmol Vis Sci.* 1997;38:1321-1332.

10. van den Berg TJ, Spekreijse H. Near infrared light absorption in the human eye media. *Vision Res.* 1997;37:249-253.
11. Unterhuber A, Povazay B, Hermann B, Sattmann H, Chavez-Pirson A, Drexler W. In vivo retinal optical coherence tomography at 1040 nm: enhanced penetration into the choroid. *Opt Express.* 2005;13:3252-3258.
12. American National Standard Institute. *American National Standard for Safe Use of Lasers.* New York: Author; 2000.
13. Wojtkowski M, Bajraszewski T, Gorczynska I, et al. Ophthalmic imaging by spectral optical coherence tomography. *Am J Ophthalmol.* 2004;138:412-419.
14. Wojtkowski M, Srinivasan V, Fujimoto JG, et al. Three-dimensional retinal imaging with high-speed ultrahigh-resolution optical coherence tomography. *Ophthalmology.* 2005;112:1734-1746.
15. Lee EC, de Boer JF, Mujat M, Lim H, Yun SH. In vivo optical frequency domain imaging of human retina and choroid. *Opt Express.* 2006;14:4403-4411.
16. Srinivasan V, Adler D, Chen Y, et al. Ultrahigh-speed optical coherence tomography for three-dimensional and en face imaging of the retina and optic nerve head. *Invest Ophthalmol Vis Sci.* 2008;49:5103-5110.
17. Yasuno Y, Hong Y, Makita S, et al. In vivo high-contrast imaging of deep posterior eye by 1-microm swept source optical coherence tomography and scattering optical coherence angiography. *Opt Express.* 2007;15:6121-6139.
18. Huber R, Adler DC, Srinivasan VJ, Fujimoto JG. Fourier domain mode locking at 1050 nm for ultra-high-speed optical coherence tomography of the human retina at 236,000 axial scans per second. *Opt Lett.* 2007;32:2049-2051.
19. Povazay B, Hermann B, Hofer B, et al. Wide field optical coherence tomography of the choroid in vivo. *Invest Ophthalmol Vis Sci.* 2008;50:1856-1863.
20. Bron AJ, Tripathi RC, Tripathi BJ. *Wolff's Anatomy of the Eye and Orbit,* 8th ed. London, UK: Hodder Arnold; 1997.
21. Povazay B, Bizheva K, Hermann B, et al. Enhanced visualization of choroidal vessels using ultrahigh resolution ophthalmic OCT at 1050 nm. *Opt Express.* 2003;11:1980-1986.
22. Kiel JW, van Heuven WA. Ocular perfusion pressure and choroidal blood flow in the rabbit. *Invest Ophthalmol Vis Sci.* 1995;36:579-585.
23. Spaide RF, Koizumi H, Pozzoni MC. Enhanced depth imaging spectral-domain optical coherence tomography. *Am J Ophthalmol.* 2008;146:496-500. Erratum in: *Am J Ophthalmol.* 2009;147:325.
24. Margolis R, Spaide RF. A pilot study of enhanced depth imaging optical coherence tomography of the choroid in normal eyes. *Am J Ophthalmol.* 2009;147:811-815.
25. Esmaeelpour M, Povazay B, Hermann B, et al. Three-dimensional 1060-nm OCT: choroidal thickness maps in normal subjects and improved posterior segment visualization in cataract patients. *Invest Ophthalmol Vis Sci.* 2010;51:5260-5266.
26. Ikuno Y, Kawaguchi K, Nouchi T, Yasuno Y. Choroidal thickness in healthy Japanese subjects. *Invest Ophthalmol Vis Sci.* 2010;51:2173-2176.
27. van Velthoven ME, van der Linden MH, de Smet MD, Faber DJ, Verbraak FD. Influence of cataract on optical coherence tomography image quality and retinal thickness. *Br J Ophthalmol.* 2006;90:1259-1262.
28. Povazay B, Hermann B, Unterhuber A, et al. Three-dimensional optical coherence tomography at 1050 nm versus 800 nm in retinal pathologies: enhanced performance and choroidal penetration in cataract patients. *J Biomed Opt.* 2007;12:041211.
29. de Bruin DM, Burnes DL, Loewenstein J, et al. In vivo three-dimensional imaging of neovascular age-related macular degeneration using optical frequency domain imaging at 1050 nm. *Invest Ophthalmol Vis Sci.* 2008;49:4545-4552.
30. Yasuno Y, Miura M, Kawana K, et al. Visualization of sub-retinal pigment epithelium morphologies of exudative macular diseases by high-penetration optical coherence tomography. *Invest Ophthalmol Vis Sci.* 2009;50:405-413.
31. Green WR, Enger C. Age-related macular degeneration histopathologic studies. The 1992 Lorenz E. Zimmerman Lecture. *Ophthalmology.* 1993;100:1519-1535.
32. Green WR, Key SN. Senile macular degeneration: a histopathologic study, 1977. *Retina.* 2005;25(5 suppl):180-250.
33. Spaide RF. Age-related choroidal atrophy. *Am J Ophthalmol.* 2009;147:801-810.
34. Wang M, Munch IC, Hasler PW, Prunte C, Larsen M. Central serous chorioretinopathy. *Acta Ophthalmol.* 2008;86:126-145.
35. Imamura Y, Fujiwara T, Margolis R, Spaide RF. Enhanced depth imaging optical coherence tomography of the choroid in central serous chorioretinopathy. *Retina.* 2009;29:1469-1473.
36. Maruko I, Iida T, Sugano Y, Ojima A, Ogasawara M, Spaide RF. Subfoveal choroidal thickness after treatment of central serous chorioretinopathy. *Ophthalmology.* 2010;117:1792-1799.
37. Yasuno Y, Okamoto F, Kawana K, Yatagai T, Oshika T. Investigation of multifocal choroiditis with panuveitis by three-dimensional high-penetration optical coherence tomography. *J Biophotonics.* 2009;2:435-441.
38. Coleman DJ, Silverman RH, Chabi A, et al. High-resolution ultrasonic imaging of the posterior segment. *Ophthalmology.* 2004;111:1344-1351.
39. Leung CK, Weinreb RN. Anterior chamber angle imaging with optical coherence tomography [published online ahead of print January 14, 2011]. *Eye.*
40. Bizheva K, Pflug R, Hermann B, et al. Optophysiology: depth-resolved probing of retinal physiology with functional ultrahigh-resolution optical coherence tomography. *Proc Natl Acad Sci U S A.* 2006;103:5066-5071.